ACS Macro Letters

Letter

pubs.acs.org/macroletters

Extensional Relaxation Times of Dilute, Aqueous Polymer Solutions

Jelena Dinic, Yiran Zhang, Leidy Nallely Jimenez, and Vivek Sharma*

Department of Chemical Engineering, University of Illinois at Chicago, Chicago, Illinois 60607, United States

Supporting Information

ABSTRACT: We show that visualization and analysis of capillary-driven thinning and pinch-off dynamics of the columnar neck in an asymmetric liquid bridge created by dripping-onto-substrate can be used for characterizing the extensional rheology of complex fluids. Using a particular example of dilute, aqueous PEO solutions, we show the measurement of both the extensional relaxation time and extensional viscosity of weakly elastic, polymeric complex fluids with low shear viscosity $\eta < 20$ mPa·s and relatively short relaxation time, $\lambda < 1$ ms. Characterization of elastic effects and extensional relaxation times in these dilute solutions is beyond the range measurable in the standard geometries used in commercially available shear and extensional rheometers (including CaBER, capillary breakup extensional rheometer). As the radius of the neck that connects a sessile drop to a nozzle is detected optically, and the extensional response for viscoelastic fluids is characterized by analyzing their elastocapillary self-thinning, we refer to this technique as optically-detected elastocapillary self-thinning dripping-onto-substrate (ODES-DOS) extensional rheometry.

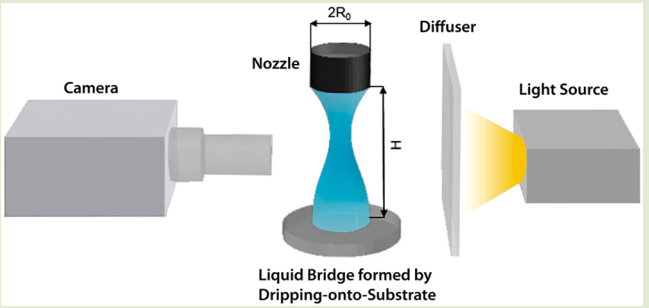

Addition of a dilute amount, even 1−400 ppm (parts per million), of a high molecular weight polymer like poly(ethylene oxide) (PEO, $M_w > 10^6$ g/mol) to a solvent like water is observed to significantly change the fluid response to extensional or stretching flows.[1] Examples include enhanced pressure drop in porous media flows,[1a] suppression of rebound in drop impact studies,[2] a discernible birefringence around a stagnation point in cross-slot flows,[3] delayed breakup in dripping, spraying or jetting,[1b,4] and possibly turbulent drag reduction.[5] The influence of polymers is even more remarkable for dilute, aqueous solutions as the measured shear viscosity $\eta(\dot{\gamma})$ appears to be Newtonian, and elastic modulus, relaxation time, and the first normal stress difference are not measured, or manifested, in steady shear or oscillatory shear tests carried out on the state-of-the-art torsional rheometers.[6]

Macromolecular solutions typically exhibit a large and measurable resistance called extensional viscosity, η_E, to streamwise velocity gradients characteristic of extensional flows[1b,7] and undergo stress relaxation with a characteristic extensional relaxation time λ_E. However, for dilute, aqueous solutions, quantitative measurements of both η_E and λ_E remain beyond the capability of commercially available devices like CaBER (capillary breakup extensional rheometer). A countable few measurements of extensional relaxation time in dilute aqueous solutions presented in the recent literature[6,7d] require bespoke instrumentation not available or easily replicable in most laboratories. The aim of the present study is 3-fold: to describe an extensional rheometry protocol that can be recreated virtually in any laboratory (quite inexpensively for high viscosity fluids), to characterize the extensional viscosity and extensional relaxation time for dilute, aqueous polymer solutions, and to provide a scaling argument that captures the concentration-dependent variation of extensional relaxation time.

Free surface flows of polymer solutions—underlying drop formation and liquid transfer in jetting and printing,[1b,4,6] dripping,[1b,4b,8] and microfluidic drop/particle production[9]—involve the formation of columnar necks that spontaneously undergo capillary-driven instability, thinning, and pinch-off. The progressive self-thinning of the neck is often characterized by self-similar profiles and scaling laws that depend on the relative magnitude of capillary, inertial, and viscous stresses for simple (Newtonian and inelastic) fluids.[1b,4] Macromolecular stretching and orientation in response to extensional flow field within the thinning columnar necks (recently visualized using DNA solutions[10]) leads to extra viscoelastic stresses that change the thinning and pinch-off dynamics.[1b]

Pioneering studies by Schümmer and Tebel[11] as well as Entov, Yarin, and collaborators[12] developed the idea of characterizing capillary-driven thinning for evaluating the role of added polymers in terms of an extensional viscosity and an extensional relaxation time. The extensional relaxation time, λ_E, is distinct and often larger in magnitude than the value of relaxation time obtained in oscillatory shear or stress relaxation experiments.[1,12] Such extensional rheometry measurements are realized in several prototypical geometries:[1b,8] (I) Dripping, where the pinch-off results from an interplay of gravitational drainage and capillarity.[8,13] (II) Jetting, where convective

Received: June 13, 2015
Accepted: July 10, 2015

DOI: 10.1021/acsmacrolett.5b00393
ACS Macro Lett. 2015, 4, 804−808

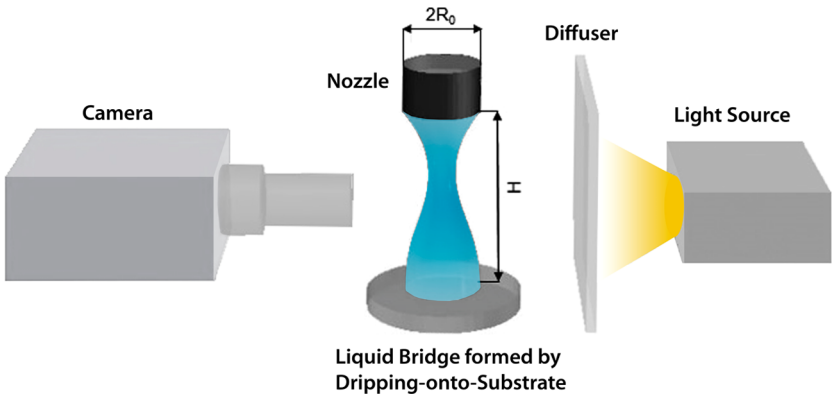

Figure 1. Introducing optically-detected elastocapillary self-thinning dripping-onto-substrate [ODES-DOS] extensional rheometry. Self-thinning dynamics of the necked region in a stretched liquid bridge formed by dripping-onto-substrate are captured using an imaging system (a light source, a diffuser, and a camera). Extensional viscosity and extensional relaxation time can be obtained from the analysis of neck-thinning dynamics.

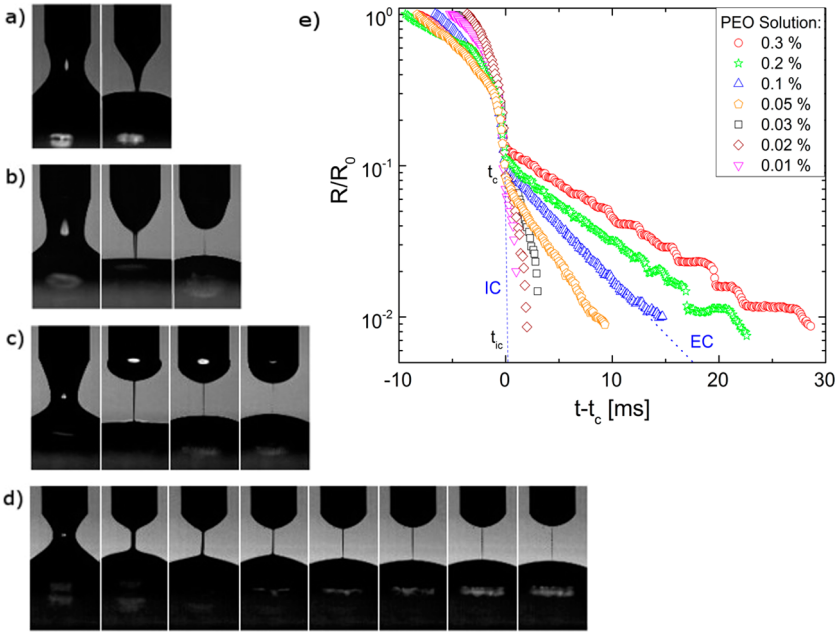

Figure 2. Image sequences and radius evolution plots obtained using the ODES-DOS method. Images, 3 ms apart, show capillary-driven thinning and breakup of a stretched liquid bridge for aqueous PEO solutions, $M_w = 10^6$ g/mol: (a) $c = 0$ wt. % (pure water), (b) $c = 0.02$ wt. %, (c) $c = 0.1$ wt. %, and (d) $c = 0.2$ wt. % ($c/c^* = 0$, 0.01, 0.45, and 1.1), respectively. (e) Radius evolution plots obtained using the ODES-DOS method are shown with the time axis shifted such that the transition point t_c overlaps. Radius evolution (blue, squares) for an aqueous $c = 0.1$ wt % PEO solution shows two distinct regimes: inertio-capillary regime, fit by eq 1 (blue dashed line) before t_c and elasto-capillary regime described by eq 2 (blue dotted line) after t_c.

instability develops on a fluid jet and the Rayleigh Ohnesorge jetting extensional rheometer (ROJER) measurements and analysis are based on understanding of the nonlinear fluid dynamics underlying the jetting process.[6,11,14] (III) Self-thinning of a stretched liquid bridge[12a−d] formed by applying a discrete step-strain to a drop between two parallel plates, and utilized in CaBER.[1b,15]

In this letter, we show that visualizing and analyzing thinning of a stretched liquid bridge formed by dripping-onto-substrate (see Figure 1) can be used for extensional rheometry characterization. As an extreme application of the dripping-onto-substrate protocol and to outline its efficacy, we carry out measurements of extensional relaxation time and extensional viscosity for low viscosity ($\eta < 20$ mPa·s), low elasticity fluids ($\lambda < 1$ ms). Such measurements are inaccessible in a standard CaBER as the pinch-off is completed even before the typical commercial instruments can stretch the liquid bridge.[1b,6,7d,15a] Campo-Deano and Clasen[7d] recently modified the CaBER protocol to create the slow retraction method (SRM) to access shorter relaxation times. But the initial step-strain required in both CaBER and SRM measurements can disrupt the fluid microstructure, influencing the observed extensional rheology response for highly structured fluids.[16] Jetting always requires higher flow rates than dripping, so the effect of preshear induced within the nozzle is less important in dripping-onto-substrate. The presence of substrate also averts issues associated with dripping:[13d] the released drop no longer hangs from the thinning neck, and changing drop volume/weight has no effect on dynamics. Furthermore, the fixed Eulerian location of the thinning neck facilitates visualization in contrast to dripping (higher viscosity and more viscoelastic fluids form longer necks).

DOI: 10.1021/acsmacrolett.5b00393
ACS Macro Lett. 2015, 4, 804−808

For dripping-onto-substrate experiments, a discrete fluid volume delivered at a relatively low flow rate, Q, is deposited onto a glass substrate placed at a fixed distance H below the nozzle. An unstable, stretched liquid bridge, bounded by the nozzle and a sessile drop on the substrate (see Figure 1), is formed, and its necked region undergoes capillary-driven thinning. Unlike CaBER that relies on a laser-based diameter measurement, neck shape and diameter are both extracted from movies captured at a rate of 8000−25 000 frames per second (fps). Analysis is carried out by using specially written codes in ImageJ[17] and MATLAB. The imaging system consists of a light source, a diffuser, and a Photron Fastcam SA3 high-speed camera equipped with a Nikkor 3.1X zoom lens (18−55 mm) and an additional super macrolens. Each measurement is repeated at least five times for the chosen nozzle (diameter: inner, D_i = 0.838 mm and outer, D_o = 1.270 mm), aspect ratio (H/D_i = 3), and dispensing rate, and a good reproducibility is observed (see Supporting Information). As the neck radius is optically detected, and the elongational viscosity as well as relaxation time are deduced by an analysis of the elasto-capillary self-thinning regime (described later), we christened this method as optically-detected elastocapillary self-thinning dripping-onto-substrate (ODES-DOS) extensional rheometry.

Aqueous solutions of PEO (Sigma-Aldrich, average molecular weight M_w = 1.0 × 10^6 g/mol) were prepared by successively diluting a stock solution (0.4% PEO in water), prepared by slowly adding polymer powder to deionized water. The solutions are placed on a roller for at least 5 days to achieve homogeneous mixing. High deformation rate mixers and flows were avoided as these are known to cause chain scission.[18] In shear rheology, solutions are considered dilute if $c/c^* < 1$, and for such solutions, the concentration-dependent solution shear viscosity $\eta = \eta_s(1 + c/c^*)$ is comparable to solvent viscosity, η_s. Here the critical overlap concentration (c^* = 0.17 wt %), i.e., the concentration value at which unperturbed polymer coils start to overlap, was computed using the formula $c^*[\eta] \approx 1$, together with Mark−Houwink−Sakurada equation: $[\eta] = KM_w^a$. Intrinsic viscosity, $[\eta]$, depends on M_w, and for PEO, the values of coefficient K = 1.25 × 10^{-2} mL/g and the exponent a = 0.78 are listed in the polymer handbook data.[19] ODES-DOS extensional rheometry characterization was carried out for PEO solutions, with concentration c = 0.005−0.3 wt % spanning a range above and below c^*.

Representative snapshots of the stretched liquid bridge formed by dripping-onto-substrate and the necked region undergoing thinning are shown in Figure 2. For pure water, the progressive thinning of neck results in the formation of a cone-shaped morphology (Figure 2a), displaying a characteristic feature of the potential flow solution obtained for inviscid fluids.[13e,20] A distinct slender liquid filament appears for polymer solutions (see Figure 2c−d), and often beads-on-a-string structures can be observed in the last stages of thinning (e.g., see Movie, included as Supporting Information). Clasen et al.[21] and Bhat et al.[22] showed that the region where the viscoelastic filament thread connects with the drop develops a sharp corner that evolves self-similarly. Qualitatively similar corner profiles are observed for polymer solutions (see Figure 2c−d). The image sequences obtained by the DOS setup were analyzed to track thinning of the neck radius over time. Two distinct regimes can be observed for the PEO solutions: an initial power law regime, followed by a slower exponential decay.

The initial neck-thinning dynamics, dominated by inertial and capillary stresses only, can be described quite well by the following expression for inertio-capillary (IC) scaling[20]

$$\frac{R(t)}{R_0} = 0.8\left(\frac{t_{ic} - t}{t_R}\right)^{2/3} \tag{1}$$

Here t_{ic} represents the pinch-off time; $R(t = 0) = R_0$ is initial radius; and ρ and σ are density and surface tension of the fluid, respectively. Here Rayleigh time $t_R = (\rho R_0^3/\sigma)^{1/2}$ is a characteristic time scale for phenomena dominated by the interplay of capillarity and inertia. A critical time for breakup t_{ic} = 1.95t_R can be computed based on eq 1. For polymer solutions, elastic effects dictate thinning dynamics after t_c (and $t_c \neq t_{ic}$), but inertio-capillary scaling (see the dashed line labeled IC, Figure 2e) is observed before t_c. The observed IC scaling is clearly distinct from the linear evolution expected for a viscous fluid $R(t)/R_0 = 1-0.07(t/t_{vc})$, in which case the characteristic time is defined as visco-capillary (VC) time $t_{vc} = \eta R_0/\sigma$. For PEO solutions used herewith, the dimensionless ratio of two time scales, known as Ohnesorge number, Oh = $t_{vc}/t_{ic} = \eta/(\rho\sigma R_0)^{1/2}$, is very small (Oh ≪ 1), implying that the inertial effects dominate over viscous contributions, as observed. We have verified experimentally that for fluids with Oh > 1 the thinning dynamics is captured by visco-capillary scaling (e.g., Supporting Information).

The elastocapillary thinning dynamics can be described using the following expression based on a theory developed by Entov and Hinch[12a]

$$\frac{R(t)}{R_0} = \sum_i \left(\frac{g_i R_0}{2\sigma}\right)^{1/3} \exp[-t/3\lambda_i] \approx \left(\frac{GR_0}{2\sigma}\right)^{1/3} \exp[-t/3\lambda_E] \tag{2}$$

Here g_i and λ_i are modulus and relaxation time that correspond to the ith mode of the relaxation spectrum.[12a] For many polymer solutions,[1b,12a] this response can be captured reasonably well by a single exponential relaxation function, where G and λ_E are the elastic modulus and the extensional relaxation time, respectively. Radius evolution in the elastocapillary regime (exponential decay, see eq 2) appears as linear on a semilog plot (see Figure 2e). While the inertio-capillary dynamics manifested before the transition point appear to be nearly concentration-independent, the lifetime of the elastocapillary regime and the total time for breakup increase with an increase in the polymer concentration.

Elastic and capillary stresses dominate the overall stress balance within the thinning filament in the elastocapillary regime. Polymer stretching, orientation, and conformational changes contribute additional tensile elastic stresses, $\eta_E\dot{\varepsilon}$, in the neck that opposes the capillary stress, σ/R. Though extensional viscosity, η_E, is only a factor of 3 times larger than the shear viscosity for Newtonian fluids, the Trouton ratio, Tr = η_E/η can be orders of magnitude higher (Tr: 10^1−10^5) for polymeric solutions.[3b,6a,7e,23] The strength of extensional flows that accompany the progressive thinning of neck can be quantified in terms of an extension rate, $\dot{\varepsilon} = -2\mathrm{d}\ \ln\ R(t)/\mathrm{d}t$. The extensional viscosity can be evaluated using the following formula

DOI: 10.1021/acsmacrolett.5b00393
ACS Macro Lett. 2015, 4, 804−808

$$\eta_E = \frac{\sigma}{\dot{\varepsilon}R} = \frac{\sigma}{-2dR(t)/dt} \quad (3)$$

The ODES-DOS technique, like most other extensional rheometry techniques,[1b,7b,24] yields a measurement of a transient extensional viscosity, $\eta_E^+(\dot{\varepsilon},\varepsilon,t)$. It is well-known that extensional viscosity exhibits a strong dependence on flow parameters[1b,7b] including strain rate, total fluid strain (ε), and the overall deformation history. For inviscid fluids, the extension rate $\dot{\varepsilon}_{ic} = (t_{ic} - t)^{-1}$ diverges as the pinch-off point is approached. However, for polymeric solutions, the elastic stresses manifested beyond t_c prevent an unbounded growth in extension rate. A constant but fairly large extension rate ($\dot{\varepsilon} = O(10^2 - 10^4)$ s^{-1}) set entirely by the intrinsic polymer dynamics is manifested in the elastocapillary regime. The Hencky strain, $\varepsilon = 2\ln(R_0/R(t))$, however, increases with time, and therefore, it is appropriate to plot extensional viscosity as a function of increasing strain, as shown in Figure 3. Increase in polymer fraction leads to an increase in both extensional viscosity and the total strain reached before pinch-off. As the shear viscosity of these dilute aqueous solutions is $1 < \eta \leq 2$ mPa·s, high Trouton ratios Tr = 10^2–10^5 are manifested in these experiments.

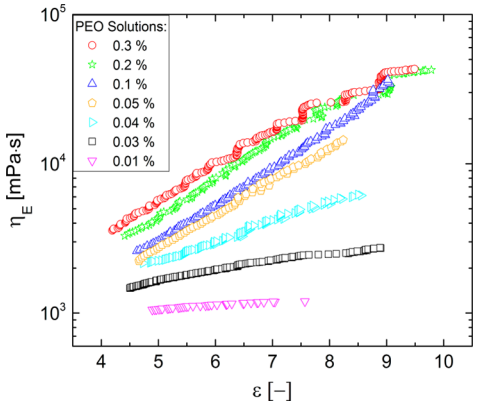

Figure 3. Extensional viscosity as a function of Hencky strain for aqueous PEO solutions obtained using ODES-DOS extensional rheometry. The polymer solutions show a significant amount of strain-hardening, and the extensional viscosity values are 10^3–10^5 times higher than the corresponding shear viscosity values for these PEO solutions.

The elastocapillary thinning regime in radius evolution data (displayed in Figure 2e) can be analyzed using eq 2 to determine the extensional relaxation time for these PEO solutions. The concentration-dependent λ_E ranges between 0.37 and 3.5 ms (see Figure 4), and all λ_E values are 3–100 times greater than the Zimm relaxation time, $\lambda_Z = 0.463([\eta]-\eta_s M_w/RT) = 0.1$ ms. The Zimm model[25] that accounts for intrachain hydrodynamic interaction and excluded volume effects is often used for describing dynamics of noninteracting coils of flexible polymers at infinite dilution. For dilute solutions ($c/c^* < 1$), Muthukumar and Freed[26] deduced a linear concentration dependence: $\lambda(c) = \lambda_{RZ}(1 + k_H[\eta]c)$, where k_H is the Huggins constant. However, the measured extensional relaxation time increases with concentration as $\lambda_E \propto \phi^{0.65}$. While polymer coils are only slightly perturbed in a strong shear flow field, macromolecules can completely unravel under a strong extensional field, leading to coil–stretch transition[3a,7e,10b,25b,27] and even to chain scission under extreme deformations.[3a,18] Though it is well-understood that stretching, uncoiling, and orientation of macromolecules change their relaxation dynamics, the observed concentration dependence, $\lambda_E \propto \phi^{0.65}$, has remained an unsolved problem.[1b,13b,28]

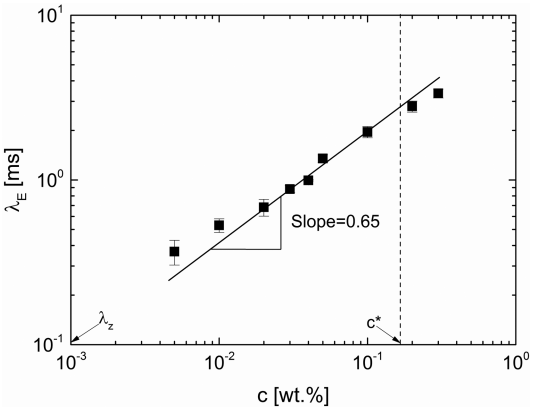

Figure 4. Extensional relaxation time λ_E as a function of concentration, c, for dilute, aqueous PEO solutions. The overlap concentration c^* and the Zimm relaxation time, λ_Z, computed for unperturbed coils, are also shown.

We postulate here that the dynamics of stretched macromolecules are similar to dynamics of unstretched chains in semidilute solutions and can be described by a scaling law deduced as follows. As the pervaded volume of stretched chain is much larger than that of unperturbed coils, substantial overlap is possible even for solutions considered dilute ($c/c^* < 1$) on the basis of c^* computed using dimensions of unstretched coils. In semidilute solutions, the (shear stress) relaxation time is computed for an effective chain composed of blobs of size, ξ (a screening length, see Rubinstein and Colby[29]). Rouse-like dynamics are displayed for dimensions $r > \xi$ as dynamics are many-chain like, and both excluded volume (EV) and hydrodynamic interactions (HI) are screened. However, for $r < \xi$, strong hydrodynamic interactions exist within the blobs, and excluded volume interactions can play a role. The analysis yields concentration-dependent relaxation time $\lambda \approx \lambda_o N^2 \phi^{(2-3\upsilon)/(3\upsilon-1)}$ for unentangled semidilute solution in contrast to Zimm relaxation time $\lambda_Z \approx \lambda_o N^{3\upsilon}$. Here the monomer relaxation time $\lambda_o \approx \eta_s b^3/kT$ and volume fraction $\phi = cb^3 N_{Av}/M_o$ can be evaluated using Avogadro's number N_{Av}, size of Kuhn segment b, and molecular weight of monomer M_0. For stretched chains, the excluded volume interactions will be screened only partially. But the exponent is $(2-3\upsilon)/(3\upsilon - 1) \cong 0.31$ if excluded volume interactions are included and $(2-3\upsilon)/(3\upsilon - 1) \cong 1$ if EV interactions are screened or absent. As the presence and absence of excluded volume effects leads to an effective size variation, the relaxation time of the stretched chains is likely to be a geometric mean of the two limiting values. This leads to a relationship of the form $\lambda_E \approx \lambda_o N^2 \phi^{0.65}$ that seems to quantitatively capture the concentration dependence observed for these solutions (and for similar literature data[6,13b,14]).

The minimum relaxation time measured in the current study is 0.37 ms, which is close to the limit of the imaging system used (spatial resolution of 8 μm and frames that are 0.04 ms apart). Shorter relaxation times can be measured with an imaging system with a higher spatiotemporal resolution. Since a regular DSLR camera, with 60 fps motion capture capability, can be used for characterizing extensional rheometry response

DOI: 10.1021/acsmacrolett.5b00393
ACS Macro Lett. 2015, 4, 804–808

for higher viscosity fluids (see Supporting Information for an example), the ODES-DOS method is both inexpensive and easily replicable. Several recent theory and simulations papers[27a,d,e,28,30] suggest that more experiments on model polymers (e.g., polyelectrolytes, branched, and semiflexible polymers) are needed for developing a robust description of macromolecular dynamics in extensional flow fields. We hope that the ODES-DOS extensional rheometry will provide easier and universal access to such measurements for model polymer solutions and for assessing sprayability, jettability, spinnability, and printability of complex fluids.

■ ASSOCIATED CONTENT

Supporting Information

Figures S1−S4 and movie. The Supporting Information is available free of charge on the ACS Publications website at DOI: 10.1021/acsmacrolett.5b00393.

■ AUTHOR INFORMATION

Corresponding Author

*E-mail: viveks@uic.edu.

Notes

The authors declare no competing financial interest.

■ REFERENCES

(1) (a) Nguyen, T. Q.; Kausch, H. H. *Flexible polymer chains in elongational flow: Theory and experiment*; Springer-Verlag: Berlin, 1999. (b) McKinley, G. H. *Rheology Reviews* **2005**, 1−48.

(2) Bergeron, V.; Bonn, D.; Martin, J. Y.; Vovelle, L. *Nature* **2000**, *405* (6788), 772−775.

(3) (a) Keller, A.; Odell, J. *Colloid Polym. Sci.* **1985**, *263* (3), 181−201. (b) Haward, S. J.; Sharma, V.; Odell, J. A. *Soft Matter* **2011**, *7* (21), 9908−9921.

(4) (a) Eggers, J.; Villermaux, E. *Rep. Prog. Phys.* **2008**, *71* (3), 036601. (b) Eggers, J. *Rev. Mod. Phys.* **1997**, *69* (3), 865−929.

(5) Graham, M. D. *Phys. Fluids* **2014**, *26* (10), 101301.

(6) (a) Sharma, V.; Haward, S. J.; Serdy, J.; Keshavarz, B.; Soderlund, A.; Threlfall-Holmes, P.; McKinley, G. H. *Soft Matter* **2015**, *11*, 3251. (b) Keshavarz, B.; Sharma, V.; Houze, E. C.; Koerner, M. R.; Moore, J. R.; Cotts, P. M.; Threlfall-Holmes, P.; McKinley, G. H. *J. Non-Newtonian Fluid Mech.* **2015**, *222*, 171.

(7) (a) Sridhar, T.; Tirtaatmadja, V.; Nguyen, D.; Gupta, R. *J. Non-Newtonian Fluid Mech.* **1991**, *40* (3), 271−280. (b) McKinley, G. H.; Sridhar, T. *Annu. Rev. Fluid Mech.* **2002**, *34*, 375−415. (c) Clasen, C.; Plog, J. P.; Kulicke, W. M.; Owens, M.; Macosko, C.; Scriven, L. E.; Verani, M.; McKinley, G. H. *J. Rheol.* **2006**, *50* (6), 849−881. (d) Campo-Deano, L.; Clasen, C. *J. Non-Newtonian Fluid Mech.* **2010**, *165* (23), 1688−1699. (e) Odell, J. A.; Carrington, S. P. *J. Non-Newtonian Fluid Mech.* **2006**, *137*, 110−120.

(8) Basaran, O. A. *AIChE J.* **2002**, *48* (9), 1842−1848.

(9) Christopher, G. F.; Anna, S. L. *J. Phys. D: Appl. Phys.* **2007**, *40* (19), R319.

(10) (a) Juarez, G.; Arratia, P. E. *Soft Matter* **2011**, *7* (19), 9444−9452. (b) Ingremeau, F.; Kellay, H. *Phys. Rev. X* **2013**, *3* (4), 041002. (c) Mai, D. J.; Brockman, C.; Schroeder, C. M. *Soft Matter* **2012**, *8* (41), 10560−10572.

(11) (a) Schummer, P.; Tebel, K. H. *Rheol. Acta* **1982**, *21* (4−5), 514−516. (b) Schummer, P.; Tebel, K. H. *J. Non-Newtonian Fluid Mech.* **1983**, *12* (3), 331−347.

(12) (a) Entov, V. M.; Hinch, E. J. *J. Non-Newtonian Fluid Mech.* **1997**, *72*, 31−54. (b) Bazilevskii, A. V.; Entov, V. M.; Rozhkov, A. N. *Polym. Sci., Ser. A* **2001**, *43* (7), 716−726. (c) Bazilevsky, A.; Entov, V.; Rozhkov, A. Liquid filament microrheometer and some of its applications. In *Third European Rheology Conference and Golden Jubilee Meeting of the British Society of Rheology*; Elsevier: Edinburgh, UK, 1990; pp 41−43. (d) Bazilevsky, A. V.; Entov, V. M.; Rozhkov, A. N. *Fluid Dyn.* **2011**, *46* (4), 613−622. (e) Entov, V. M.; Yarin, A. L. *Fluid Dyn.* **1984**, *19* (1), 21−29. (f) Yarin, A. L. *Free Liquid Jets and Films: Hydrodynamics and Rheology*; Longman Scientific & Technical and Wiley & Sons: Harlow, New York, 1993. (g) Stelter, M.; Brenn, G.; Yarin, A. L.; Singh, R. P.; Durst, F. *J. Rheol.* **2000**, *44* (3), 595−616.

(13) (a) Amarouchene, Y.; Bonn, D.; Meunier, J.; Kellay, H. *Phys. Rev. Lett.* **2001**, *86* (16), 3558−3561. (b) Tirtaatmadja, V.; McKinley, G. H.; Cooper-White, J. J. *Phys. Fluids* **2006**, *18* (4), 043101. (c) Cooper-White, J. J.; Fagan, J. E.; Tirtaatmadja, V.; Lester, D. R.; Boger, D. V. *J. Non-Newtonian Fluid Mech.* **2002**, *106* (1), 29−59. (d) Wagner, C.; Amarouchene, Y.; Bonn, D.; Eggers, J. *Phys. Rev. Lett.* **2005**, DOI: 10.1103/PhysRevLett.95.164504. (e) Furbank, R. J.; Morris, J. F. *Int. J. Multiphase Flow* **2007**, *33* (4), 448−468.

(14) (a) Christanti, Y.; Walker, L. M. *J. Non-Newtonian Fluid Mech.* **2001**, *100* (1−3), 9−26. (b) Christanti, Y.; Walker, L. M. *J. Rheol.* **2002**, *46* (3), 733−748.

(15) (a) Rodd, L. E.; Scott, T. P.; Cooper-White, J. J.; McKinley, G. H. *Appl. Rheol.* **2005**, *15* (1), 12−27. (b) Anna, S. L.; McKinley, G. H. *J. Rheol.* **2001**, *45* (1), 115−138.

(16) (a) Miller, E.; Clasen, C.; Rothstein, J. P. *Rheol. Acta* **2009**, *48* (6), 625−639. (b) Plog, J.; Kulicke, W.; Clasen, C. *Appl. Rheol.* **2005**, *15* (1), 28−37.

(17) Schneider, C. A.; Rasband, W. S.; Eliceiri, K. W. *Nat. Methods* **2012**, *9* (7), 671−675.

(18) (a) Odell, J. A.; Keller, A.; Rabin, Y. *J. Chem. Phys.* **1988**, *88* (6), 4022−4028. (b) Odell, J. A.; Muller, A. J.; Narh, K. A.; Keller, A. *Macromolecules* **1990**, *23* (12), 3092−3103.

(19) Mark, J. E. *Polymer Data Handbook*; Oxford University Press: New York, 2009; Vol. *27*.

(20) (a) Day, R. F.; Hinch, E. J.; Lister, J. R. *Phys. Rev. Lett.* **1998**, *80* (4), 704−707. (b) Castrejón-Pita, J. R.; Castrejón-Pita, A. A.; Hinch, E. J.; Lister, J. R.; Hutchings, I. M. *Phys. Rev. E* **2012**, *86* (1), 015301. (c) Castrejón-Pita, J. R.; Hutchings, I. M., Perspective: The Breakup of Liquid Jets and the Formation of Droplets. In *Computational and Experimental Fluid Mechanics with Applications to Physics, Engineering and the Environment*; Springer: New York, 2014; pp 249−257.

(21) Clasen, C.; Eggers, J.; Fontelos, M. A.; Li, J.; McKinley, G. H. *J. Fluid Mech.* **2006**, *556*, 283−308.

(22) Bhat, P. P.; Appathurai, S.; Harris, M. T.; Basaran, O. A. *Phys. Fluids* **2012**, *24* (8), 083101.

(23) (a) Haward, S. J.; Sharma, V.; Butts, C. P.; McKinley, G. H.; Rahatekar, S. S. *Biomacromolecules* **2012**, *13* (5), 1688−1699. (b) Petrie, C. J. S. *Elongational Flows*; Pitman: London, 1979. (c) Petrie, C. J. S. *J. Non-Newtonian Fluid Mech.* **2006**, *137* (1−3), 15−23.

(24) Macosko, C. W. *Rheology: Principles, Measurements and Applications*; VCH Publishers Inc: New York, 1994.

(25) (a) Doi, M.; Edwards, S. F. *The Theory of Polymer Dynamics*; Oxford University Press: New York, 1986; p 406. (b) Larson, R. G. *J. Rheol.* **2005**, *49* (1), 1−70.

(26) Muthukumar, M.; Freed, K. F. *Macromolecules* **1978**, *11* (5), 843−852.

(27) (a) Somani, S.; Shaqfeh, E. S. G.; Prakash, J. R. *Macromolecules* **2010**, *43* (24), 10679−10691. (b) Hinch, E. J. *J. Non-Newtonian Fluid Mech.* **1994**, *54*, 209−230. (c) Perkins, T. T.; Smith, D. E.; Chu, S. *Science* **1997**, *276*, 2016−2021. (d) Schroeder, C. M.; Babcock, H. P.; Shaqfeh, E. S. G.; Chu, S. *Science* **2003**, *301* (5639), 1515−1519. (e) Schroeder, C. M.; Shaqfeh, E. S. G.; Chu, S. *Macromolecules* **2004**, *37* (24), 9242−9256. (f) Larson, R. G.; Magda, J. J. *Macromolecules* **1989**, *22* (7), 3004−3010.

(28) (a) Prabhakar, R. Enhancement of coil--stretch hysteresis by self-concentration in extensional flows, and its implications for capillary thinning of liquid bridges of dilute polymer solutions. *arXiv preprint arXiv:1404.6746*, 2014. (b) Prabhakar, R.; Prakash, J. R.; Sridhar, T. *J. Rheol.* **2006**, *50* (6), 925−947.

(29) Rubinstein, M.; Colby, R. H. *Polymer Physics*; Oxford Univ. Press: New York, 2003.

(30) Mai, D. J.; Marciel, A. B.; Sing, C. E.; Schroeder, C. M. *ACS Macro Lett.* **2015**, *4* (4), 446−452.

DOI: 10.1021/acsmacrolett.5b00393
ACS Macro Lett. 2015, 4, 804−808